



A STUDY ON APPLICATION OF SEISMIC INTERFEROMETRY TO TRAFFIC INDUCED VIBRATION

T. Hirai⁽¹⁾, H. Takahashi⁽²⁾, M. Mori⁽³⁾

⁽¹⁾ Assistant Professor, Nagoya University, hirai.takashi@nagoya-u.jp

⁽²⁾ Associate Professor, Meijo University, hirohito@meijo-u.ac.jp

⁽³⁾ Designated Professor, Nagoya University, m.mori@nagoya-u.jp

Abstract

Seismic interferometry is widely used to explore the subsurface structure. Seismic ground motions or microtremors are often used as the signal source for seismic interferometry, since the pseudo-shot records, namely Green's functions, are obtained without any artificial seismic source. In this study, the seismic interferometry is applied to obtain the pseudo-shot records using the traffic induced vibrations. It is beneficial for the subsurface exploration in the urban area to use the traffic induced vibrations, since it is found anywhere in the city.

Wapenaar and Fokkema (2006) derived the basic equation of the seismic interferometry. According to the theory, the Green's function representing the ground motion at a point due to the impulse at another point is synthesized by stacking the cross-spectra between both points in the frequency domain. Applying the method, the Green's functions for arbitrary source-receiver set can be obtained from the microtremor records. In general, very long time and many samples of the microtremor are necessary to get the Green's functions with enough accuracy.

In this study, the seismic interferometry is applied to the traffic induced vibration. It is beneficial for the subsurface exploration in the urban area to use the traffic induced vibration, since it is the dominant source of the microtremor in the urban area. Through the three cases of application, the Green's functions seem to be obtained appropriately including propagation of the first motions. Furthermore, the wave speed is estimated using the pasteup of the Green's functions for linear aligned sensors.

Keywords: seismic interferometry, traffic induced vibration, geophysical exploration, subsurface structure



1. Introduction

Understanding the subsurface structure is very important for the building designing and disaster hazard evaluation. There are many exploration methods such as standard penetration test, PS logging survey, seismic refraction survey, seismic reflection survey, and so on. These methods require the artificial seismic source. Recently, several methods based on the microtremor measurement become popular since they do not require the artificial seismic source. In particular, the seismic interferometry is useful to obtain the pseudo-shot record, namely Green's function, between arbitrary source-receiver set. However, it is necessary very long microtremor record or a lot of seismic ground motion records to obtain the Green's function with enough accuracy. If the method can be applied to the traffic induced vibration, it is useful for the subsurface exploration in the urban area, since it is found anywhere in the city. In this study, the seismic interferometry is tried to apply to three cases of the traffic induced vibrations: subway train induced vibration, Shinkansen train induced vibration, and the road traffic induced vibration. For each case, the Green's functions are estimated as the pseudo-shot records appropriately including propagation of the first motions, suggesting the wave velocities.

2. Theory

The mathematical formulations of the seismic interferometry are briefly described below. Wapenaar and Fokkema [1] derived the basis equation of the seismic interferometry as

$$2 \operatorname{Re}[G(\mathbf{x}_B, \mathbf{x}_A, \omega)] = \frac{2}{\rho c} \int_D G^*(\mathbf{x}_B, \mathbf{x}, \omega) G(\mathbf{x}_A, \mathbf{x}, \omega) dS, \quad (1)$$

where $G(\mathbf{x}_B, \mathbf{x}_A, \omega)$ denotes the Green's function in the frequency domain representing the ground motion at the point B due to the impulse at the point A. The integral is applied over the closed surface D including the point A and B. The Eq. (1) suggests that the Green's function between the points A and B is obtained by stacking a lot of cross-spectra of the ground motions at points A and B due to the source on the closed surface D . If the sources are localized on the line C , the surface integral in the Eq. (1) is replaced by the line integral along C as

$$2 \operatorname{Re}[G(\mathbf{x}_B, \mathbf{x}_A, \omega)] \propto \frac{2}{\rho c} \int_C G^*(\mathbf{x}_B, \mathbf{x}, \omega) G(\mathbf{x}_A, \mathbf{x}, \omega) ds. \quad (2)$$

In general, the traffic vibration sources seem to be localized along the railway or the road. In this study, the Green's functions are estimated by stacking the cross-spectra of the traffic induced vibration records based on the Eq. (2), assuming the integral path C corresponds to the railway or the road. The cross-spectrum is computed in the deconvolution form by Vasconcelos and Snieder [2] as

$$R(\mathbf{x}_B, \mathbf{x}_A, \mathbf{x}, \omega) = \frac{G^*(\mathbf{x}_B, \mathbf{x}, \omega) G(\mathbf{x}_A, \mathbf{x}, \omega)}{[G^*(\mathbf{x}_A, \mathbf{x}, \omega) G(\mathbf{x}_A, \mathbf{x}, \omega)]^* W(\omega)}, \quad (3)$$

in order to remove the source characteristics. In Eq. (3), the denominator is smoothed by the Parzen window $W(\omega)$ with the frequency band of 0.05 Hz. Therefore, the time series of the Green's function between points A and B is estimated as

$$G(\mathbf{x}_B, \mathbf{x}_A, \omega) = \sum R(\mathbf{x}_B, \mathbf{x}_A, \mathbf{x}, \omega), \quad (4)$$

where the summation is applied over all samples of the traffic induced vibrations.



Fig. 1 – Sensor placement for the measurement of the subway train induced vibration



Fig. 2 – Sensor placement for the measurement of the Shinkansen train induced vibration

3. Measurements

In this study, the seismic interferometry is applied to three cases of the traffic induced vibration: the subway train induced vibration, the Shinkansen train induced vibration, and the road traffic induced vibration.

3.1 Subway train induced vibration

Fig. 1 shows the sensor placement for the measurement of the subway train induced vibration. The microtremor including the subway train induced vibrations was measured above the Meijo line, Nagoya City subway, Japan, dividing the three sections: northern part, central part, and southern part. The vibration was measured by 18 sensors aligned linearly with the interval of 5 m at same time.



Fig. 3 – Sensor placement for the measurement of the road traffic induced vibration

3.2 Shinkansen train induced vibration

Fig. 2 shows the sensor placement for the measurement of the Shinkansen train induced vibration. The microtremor including the Shinkansen train induced vibrations was measured along the viaduct of the Tokaido Shinkansen. The vibration was measured by 21 sensors aligned linearly with the interval of 5 m at same time.

3.3 Road traffic induced vibration

Fig. 3 shows the sensor placement for the measurement of the road traffic induced vibration. The microtremor including the road traffic induced vibrations was measured on the sidewalk of the road along north-south direction. The vibration was measured by 43 sensors aligned linearly with the interval of 5 m at same time.

4. Results

4.1 Subway train induced vibration

Fig. 4 shows an example of the microtremor record including the subway train induced vibration. The relatively intense portion indicated by the rectangle in the panel (a) seems to be excited by the train. The absolute value of the Fourier spectra is shown in the panel (b) for the samples with and without the train induced vibration. According to the figure, the train induced vibration consists of the component about 30 Hz mainly. Fig. 5 shows the pseudo-shot records, namely the Green's functions, between arbitrary point and reference points 1, 9, and 18. The ticks of the vertical axis denote the sensor point indices. In the figure, it is shown that the characteristic phase propagates from the reference point with the almost constant velocity. The wave speed is estimated at 220 – 260 m/s from the slope of the phase. In the Fig. 5, the dominant phase is seen most clearly in the northern part. Fig. 6 shows the relation between the train speed and the distance from the station. According to the figure, the train speed is the fastest in the northern part. In this case, the faster the train, the higher the S/N ratio of the estimated Green's function.

4.2 Shinkansen train induced vibration

Fig. 7 shows an example of the microtremor record including the Shinkansen train induced vibration. The panel (b) is the enlarged view of the portion of the train passing of the panel (a). In the panel (b), there are 16 same patterns corresponding to the 16 cars of the Tokaido Shinkansen trains. This pattern causes the bright line spectrum as shown in the panel (c). Fig. 8 shows the pseudo-shot records, namely the Green's functions, between arbitrary point and reference points 1, 10, and 20. As same as Fig. 5, the wave speed is estimated at 200 – 220 m/s from the slope of the dominant phase. However, the wave propagation seen in Fig. 8 is slightly vague than that seen in Fig. 5. As shown in Fig. 7, this result may have influenced by the coherent characteristics of the Shinkansen induced vibration.

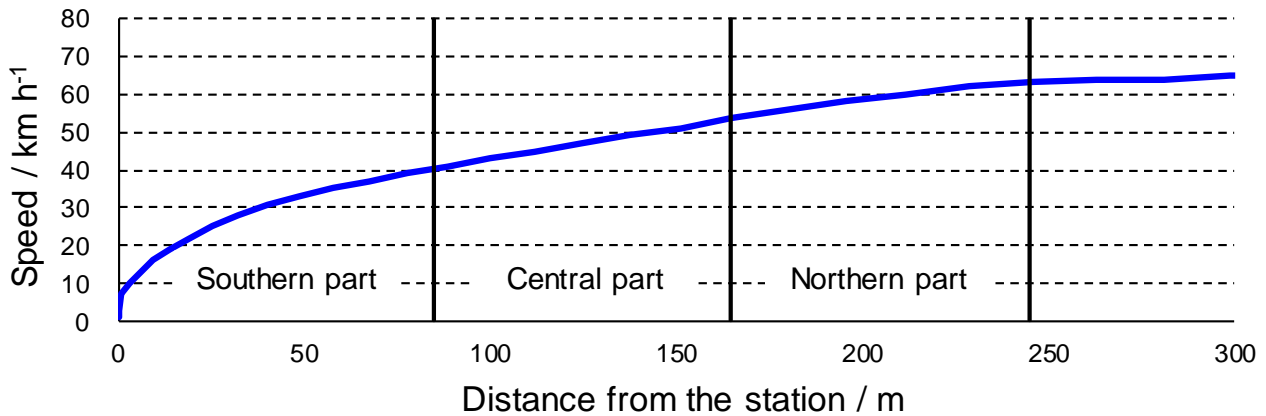


Fig. 4 – Relation between the train speed and the distance from the station

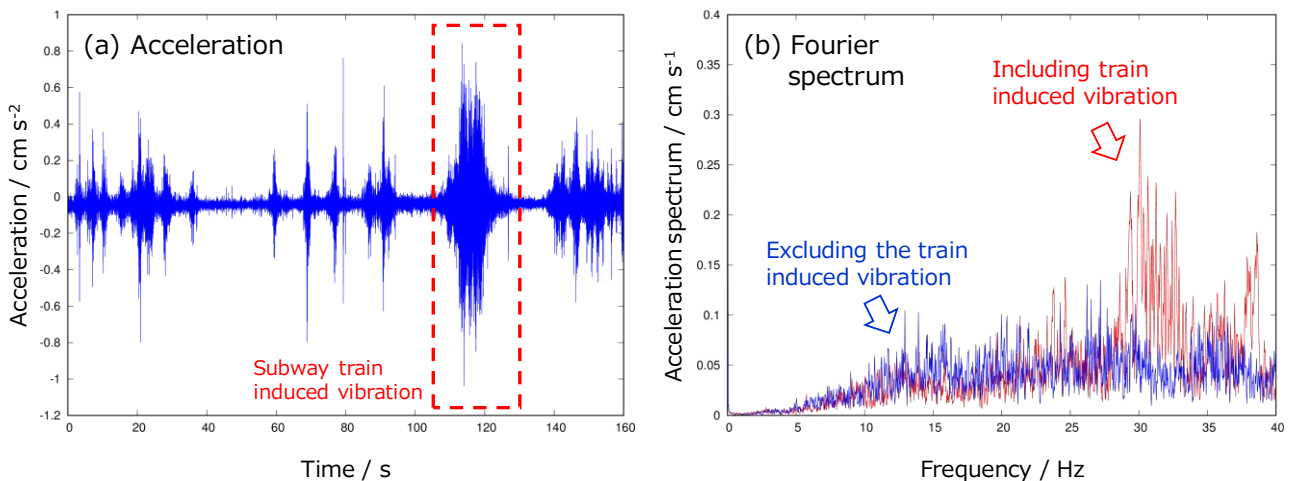


Fig. 5 – Example of the subway train induced vibration record

4.3 Road traffic induced vibration

Fig. 9 shows an example of the microtremor record including the road traffic induced vibration. Several wave groups due to the traffic vibration propagate to north and south. Fig. 10 shows the pseudo-shot records, namely the Green's functions, between arbitrary point and reference points 1, 22, and 43. As same as Fig. 5 and Fig. 8, the wave speed is estimated at 210 m/s from the slope of the dominant phase. In Fig. 10, the wave propagation seems to be the most apparently, as compared to Fig. 5 and Fig. 8. This result may have brought by the incoherent characteristics of the road traffic induced vibration, in contrast to the case of the Shinkansen train induced vibration. Fig. 11 shows the velocity profiles of P-wave and S-wave by the PS logging survey conducted near the measured site. According to the velocity profile of the S-wave, the wave speed estimated by the seismic interferometry corresponds to the S-wave velocity of the surface layer.

5. Conclusion

In this study, the seismic interferometry was applied to the three kinds of traffic induced vibration: subway train induced vibration, Shinkansen train induced vibration, and the road traffic induced vibration. As the result, the pseudo-shot record, namely the Green's function, between two points is appropriately obtained by

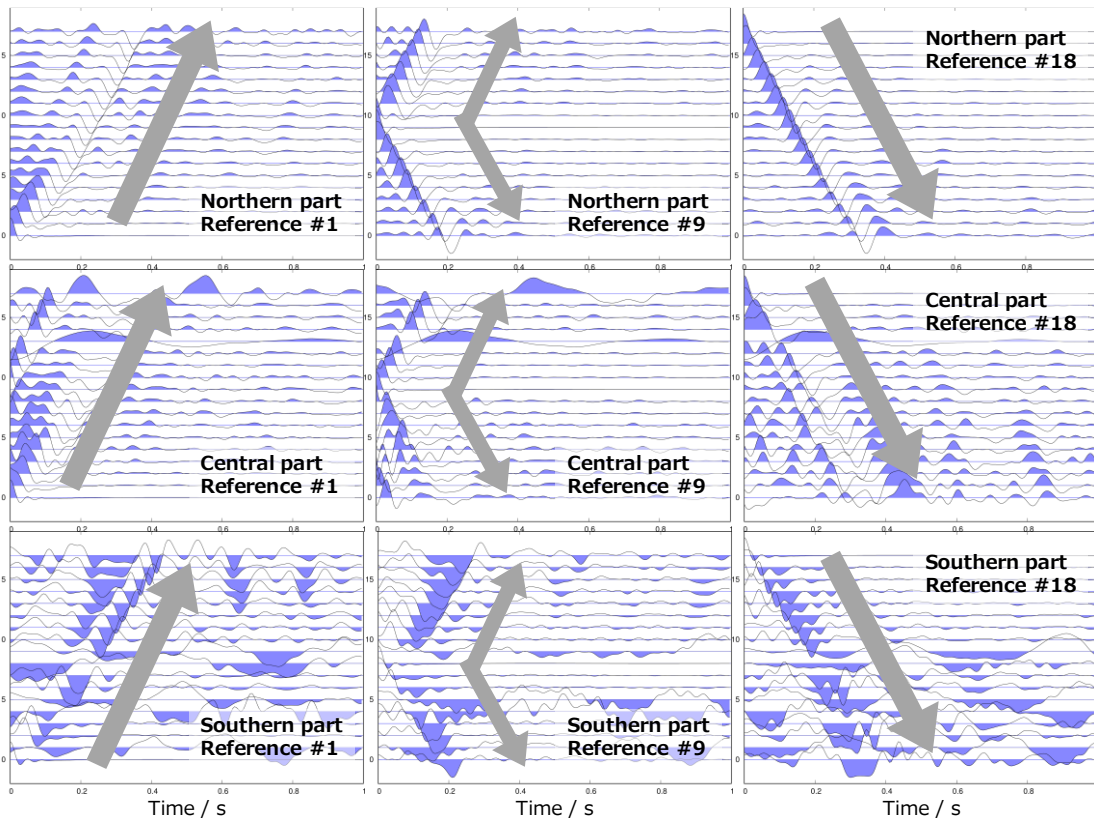


Fig. 6 – Pseudo-shot records obtained by the subway train induced vibration

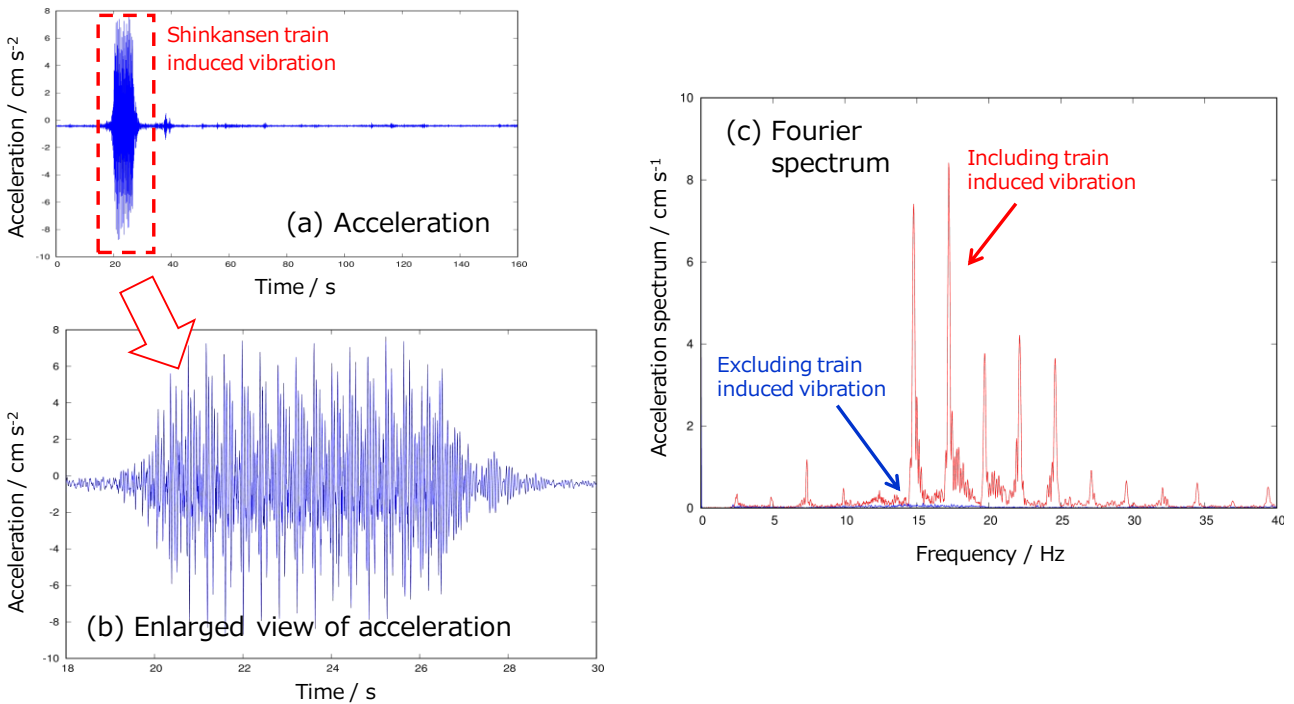


Fig. 7 – Example of the Shinkansen train induced vibration

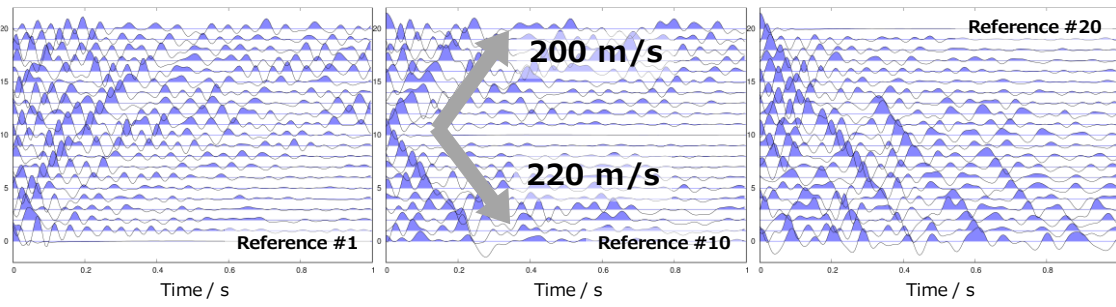


Fig. 8 – Pseudo-shot records obtained by the Shinkansen train induced vibration

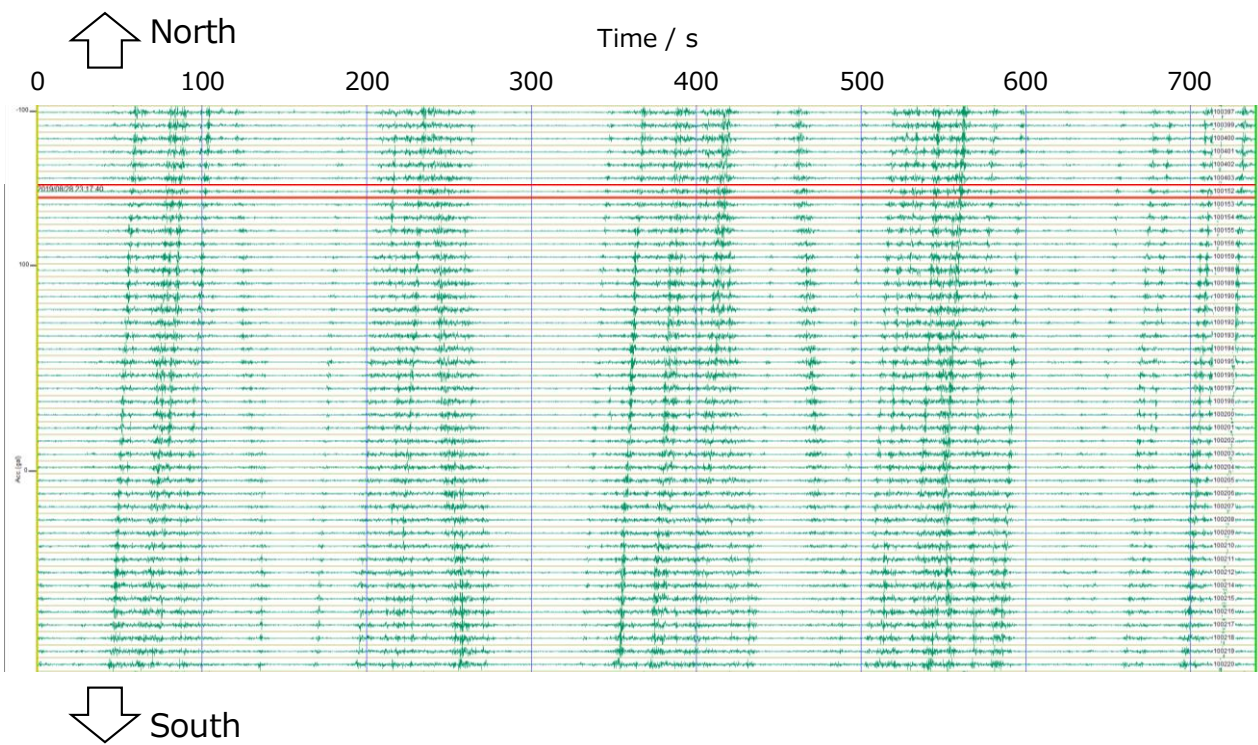


Fig. 9 – Example of the road traffic induced vibration

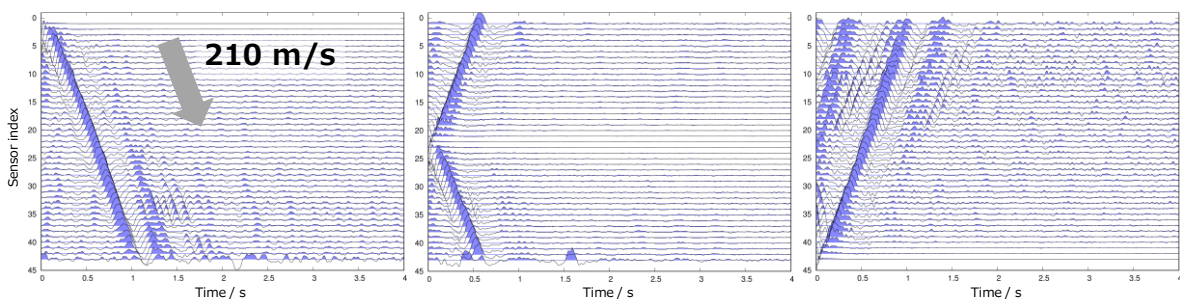


Fig. 10 – Pseudo-shot records obtained by the road traffic induced vibration

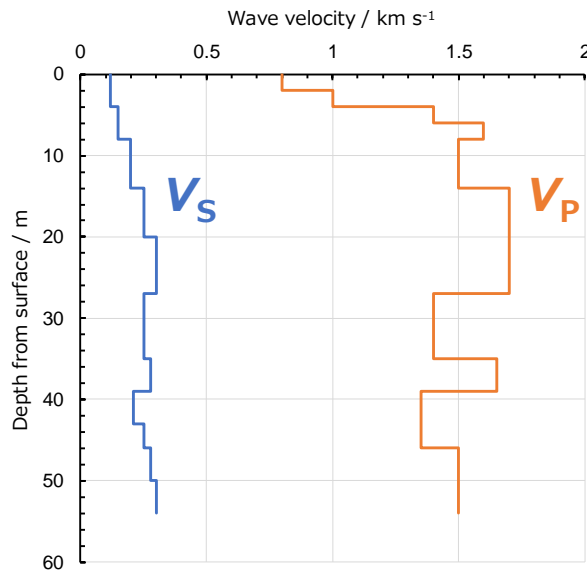


Fig. 11 – Velocity profiles of P-wave and S-wave

stacking the cross-spectra of the microtremor record including the traffic induced vibration. In addition, the wave propagation speed was estimated by using the linearly aligned sensors. The S/N ratio of obtained Green's function is higher in the case of the road traffic induced vibration than the subway and the Shinkansen train induced vibration. This result may be caused by the frequency characteristics of the vibration source.

6. Acknowledgements

This work was supported by JSPS KAKENHI Grant Numbers 18K04428 and 17K01308. The measurement of Shinkansen train induced vibration was conducted in Meiji elementary school, Nagoya, Japan. The authors appreciate the great efforts in the measurements and the analyses by then students, Ms. Hiraoka, Mr. Sakakibara, Mr. Kobayashi, Mr. Sagae, Mr. Ohta, and Mr. Sakai.

7. References

- [1] Wapenaar K, Fokkema J (2006): Green's function representations for seismic interferometry. *Geophysics*, **71**, SI33-SI46.
- [2] Vasconcelos I, Snieder R (2008): Interferometry by deconvolution, Part 1 – Theory for acoustic waves and numerical examples. *Geophysics*, **73**, S115-S128.